Multi-distributed wireless sensors for monitoring a long distance transport in a reefer container

Heidi Tatiana Jiménez-Ariza

Eva Cristina Correa

Belén Diezma and Adolfo Moya-González

Francisco Javier Arranz

Pilar Barreiro

Abstract: The study of the temperature gradients in cold stores and containers is a critical issue in the food industry for the quality assurance of products during transport and for minimising losses. This work presents an analysis of the temperatures during the refrigerated transport of 4,320 kg of blueberries in a reefer (set point temperature at –1ºC) on a container ship from Montevideo (Uruguay) to Verona (Italy). The monitoring was performed by using semi-passive RFID loggers (TurboTag cards). The objective was to carry out a multi-distributed supervision using low-cost, wireless and autonomous sensors for the characterisation of the distribution and spatial gradients of temperatures during a long distance transport. Data analysis shows spatial (phase space) and temporal sequencing diagrams and reveals a significant heterogeneity of temperature at different locations in the container, which highlights the ineffectiveness of a temperature control system based on a single sensor, as is usually done.

Keywords: RFID TurboTag loggers; transoceanic shipping; truck transport; phase diagrams; blueberries; controlled atmosphere; food.

1 Introduction

According to FAO (Gustavsson et al., 2011), roughly one-third of the edible parts of food produced for human consumption is lost or wasted globally, totalling approximately 1.3 billion tons per year. Fruits and vegetables, plus roots and tubers, have the highest wastage rates of any food, with global quantitative food losses and waste per year of 40–50%. FAO defines *food losses* as those that take place at the production, postharvest and processing stages in the food supply chain. Postharvest handling and storage, which includes losses due to spillage and degradation during handling, storage and transportation between farms and distribution, are responsible for between 5%–10% of direct losses. The report of FAO (2014) indicates that one of the pillars that should underlie the strategy for reducing losses and food waste should include the technology, innovation and training used for data collection, as well as the implementation of best practices and investments in infrastructure and capital to improve the efficiency of food systems.

In this context, the concept of *precision postharvest* can be defined as implementing the correct postharvest action at the right time and in the right place, that is, the setting of post-harvest practices to the needs of each product, reducing environmental and social impacts associated with post-harvest losses and increasing competitiveness through the greater efficiency of such practices. As in precision agriculture, the development of *precision postharvest* implies an intensification of management of information by means of sensing, data analysis and communication.

Rapid advances in sensors and wireless communications have the potential to assist in dealing with the large amount of data generated by a monitoring system. Low cost, wireless and autonomous sensors, from the point of view of power supply and recording capabilities, are the most suitable for the supervision and control of cold chambers, such as a reefer container (Costa et al., 2013; Jiménez-Ariza et al., 2014). These allow for intensive and real-time data acquisition networks, which make feasible the reconstruction of the time and spatial distribution of variables such as temperature or fluid velocity fields from point measurements (Garcia et al., 2007). Multi-distributed sensor networks have been implemented previously for the supervision of multimodal containers, characterising the thermal behavior of a container under several experimental conditions, such as cooling modes, the onset of defrosting and external temperatures by means of 69 4-wires Pt-100 (RTD) located on the walls, in the ceiling and on the floor of a reefer (Rodriguez-Bermejo et al., 2007); Jedermann et al. (2013) used 138 iButton temperature data loggers to measure the spatial temperature profile of a 40-foot reefer container of bananas by placing the sensors mainly in the boxes, either in the centre between the bananas or in the free space in the corners of the boxes; Jiménez-Ariza et al. (2014) implemented a sensor network comprising 39 TurboTag (RFID Tags) temperature sensors and 13 iButton temperature and relative humidity (RH) sensors, which were equi-spatially distributed along a load of lemons attached to the inner surface of the cartons, to study the temperature, RH and enthalpy gradients inside a 40-foot reefer container ship from Uruguay to Spain; Lang et al. (2011) proposed the concept of 'intelligent container': a container equipped with 16 sensor nodes, each with a temperature and humidity sensor, packed inside the goods.

The use of active RFID tags with temperature sensors embedded or wireless sensor nodes based on the TmoteSky/TelosB platform, which can operate as a forwarder in a multiple hop network (Lang et al., 2011), between other technologies provides the managing system with a description of the current state of the cold chain. From time data, it is possible to generate information regarding the increasing complexity, and as in precision agriculture, precision postharvest needs to integrate different levels of information. One approach is to study the time series of the variable registered by sensors by means of new tools, such as the chaotic analysis of time series and the definition of the phase space (or phase graph); its potential to display the behavior of dynamical systems of temperature and RH has been demonstrated (Correa et al., 2014; Jiménez-Ariza et al., 2014). Other authors have implemented known models for the prediction of heat and mass transfer during transportation, combining variables, such as temperature, with time dependent aspects of transportation, such as fluctuating external ambient conditions, door openings, product removal/loading, etc… (James et al., 2006), or computed complex variables, such as the psychrometric ones (Jiménez-Ariza et al., 2014). Jedermann et al. (2013) developed empirical models to explain and predict temperature changes, the emergence of warm spots or fruit shelf life. The system, developed for the 'intelligent container' project, uses several algorithms to relate temperature and quality losses, to detect malfunctioning sensors and to establish the minimum sensor density needed to provide an accurate spatial interpolation and measurement intervals through a 'cognitive system'.

The implementation of new dynamic optimal planning methodologies can overcome the hypothesis of fixed life of a perishable product by using real-time information. Integrated production and distribution planning is a recent and promising approach that

considers the fact that the supply chain is indeed a dynamic system, thus taking into account the 'time' variable (Dabbene et al., 2014).

Temperature is a well-established indicator for monitoring the transport conditions of fresh products and is the most important environmental factor affecting blueberry quality after harvest. The expansion of the blueberry global industry has made it necessary to transport the fruit in refrigerated sea containers for durations even longer than three weeks (Paniagua et al., 2014). It is known that in this type of freight reefers, significant temporal and spatial temperature gradients may occur during shipping (Jiménez-Ariza et al., 2014; Jedermann et al., 2009; James et al., 2006). According to Paniagua et al. (2014), this heterogeneity of the temperatures could constitute an important factor affecting the blueberry final quality in the marketplace.

The objective of this work is the supervision of a commercial shipping of blueberries by means of a multi-distributed net of low cost and autonomous wireless temperature sensors, through the application of a specific methodology of data analysis based on the chaotic analysis of time series, as a quick tool for the characterisation of temporal and spatial gradients of temperature in a multimodal container.

2 Materials and methods

2.1 Experimental setup

Eight pallets of 540 kg of blueberries each, loaded in a reefer of 40' (11.6 × 2.3 × 2.2 m for internal dimensions), were monitored along a multimodal ship from Montevideo (Uruguay) to Verona (Italy). The container, equipped with a controlled atmosphere system (5% O_2 and 10% CO_2), included other species to complete the load. The exact location of the eight pallets inside the container was unknown. The set point temperature was –1°C.

Figure 1 Scheme of the sensors placement in the pallets (see online version for colours)

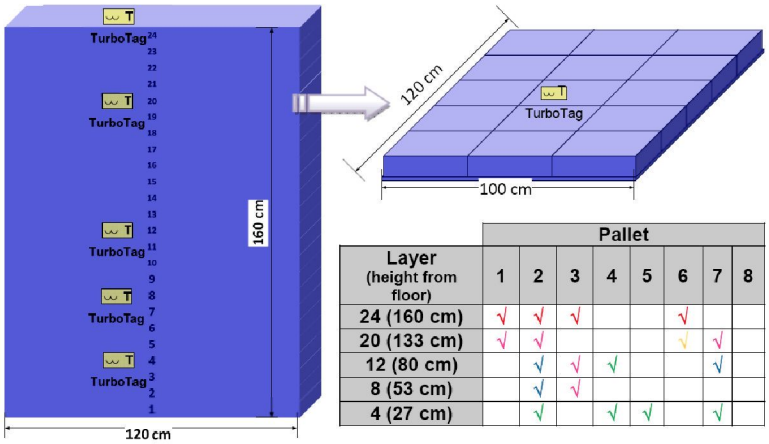

Layer (height from floor)	Pallet 1	2	3	4	5	6	7	8
24 (160 cm)	√	√	√			√		
20 (133 cm)	√	√				√	√	
12 (80 cm)		√	√	√			√	
8 (53 cm)		√	√					
4 (27 cm)		√		√	√		√	

Notes: Positions in each pallet with available temperature data are marked. The same colour code as in Figure 2 is used (same colour indicates belonging to the same sensor cluster).

Table 1 Container itinerary

Shipping by	*Way points*	*Time zone*	*Distance*	*Speed*	*Days*		*Arrival*	*Departure*
					At sea/road	*In port*		
Maersk Lins vessel	Port of Montevideo (Uruguay) to	GMT-3.0	11,629 km	12 knots	22.2	1.4	17 November 2012	19 December 2012
	Port of Rotterdam (Holland) to	GMT+ 1.0		-	-	1	12 December 2012	13 December 2012
Truck	City of Verona (Italy)	GMT+ 1.0	1,128 km	80 km/h	3	0.8	17 December 2012	
	Total		12,757 km		25.2 (88.7%)	3.2 (11.3%)		

Table 1 shows data of the complete itinerary followed by the reefer during 28.4 days. The first 24.6 days of travel (LSS – long sea shipping) were made in the Maersk Lins vessel from the port of Montevideo to the port of Rotterdam (Netherlands), and then the container was transported by truck (72 hours) from the port of Rotterdam to the fruit packinghouse in Verona (Italy) (SS – short shipping).

Boxes of corrugated carton were palletised in 24 layers with 15 boxes per layer. Each 1.5 kg box, type open tray, contained 12 perforated plastic boxes (83 mm × 80 mm × 40 mm) with 125 g of blueberries each.

The multi-distributed sensor network comprised 40 TurboTag (RFID Tags) temperature sensors, from which only 18 were recovered with correctly collected data. The distribution of the 18 tags is shown in Figure 1. The sensors were distributed amongst the load of blueberries. It was planned that in each pallet, four tags would be located inside the boxes and between the trays of blueberries at the centre of four different layers (4-8-12-20). One additional tag per pallet was placed on top of each pallet. Table 2 shows the technical characteristics of the low cost (approximately 25$ each) TurboTag® T-700 sensors. They are autonomous in power supply for at least one year, furnished with on-board data memory and very easy to affix to the load. All communications with the T-700 series tags were carried out using an RFID reader DR-1 (RFID Interface 13.56 MHz). This is a small desktop USB device for use with a PC that runs with Session Manager Software. The tag download requires 2 s on average, with an RFID read distance of approximately 5–10 cm. Due to the 702 data points of available internal memory, the temporal resolution established for TurboTag in this study was 71 min/data.

Table 2 Description of the technical characteristics of RFID sensors and of the test carried out for this work (in yellow) (see online version for colours)

Sensor range ± accuracy	*On-board data memory*	*Interface*	*Size*	*Test characteristics*		
				No. valid sensors	*No. valid data/sensor*	*Period (min/data)*
 TurboTag ® – 30°C to +40°C ±0.5°C	702	RFID at 13.56 MHz	Credit card	18	577	71

2.2 Data analysis

To facilitate the handling of data from the 18 RFID tags, a hierarchical clustering based on temporal series was performed to define groups of sensors. The matrix of Euclidean distances between each pair of individuals was calculated, grouping the closest individuals and hierarchically merging groups (or individuals) whose combination gave the smallest average linkage distance (that is, the average distance between all pairs of objects in any two clusters). A MatLab® devoted code was developed to generate groups of sensors based on the cluster tree features.

To analyse the data recorded by the RFID sensors, the reconstruction of the phase space from the time series was carried out, as outlined below. It is well known that a

continuous dynamical system can always be described by means of a system of N differential equations in canonical form

$$\frac{dy_i}{dt} = f_i\left(y_1, y_2, \ldots, y_N, t\right),$$

with i = 1, 2, N, where y_i is the i^{th} physical magnitude evolving in time t. The overall representation (y_1 y_2, …, y_N) of the corresponding N solutions $y_i(t)$ i is the so-called phase space. Notice that the behavior of the system is determined by the structure of the phase space. Following Eckmann and Ruelle [see Sec. II-G in Eckmann and Ruelle, (1985)] the best way to reconstruct the phase space from a time series is by using *time delays* [rather than the numerical time derivatives proposed by Packard et al. (1980)]. The technique is as follows. Let the experimental time series be $Y_1^{(k)} = y_1(t_k)$, with k = 1,2,M, corresponding to M periodic measures (i.e., measures with a fixed time step $\tau = t_{k+1} - t_k$) of the physical magnitude y_1. Then, we can reconstruct the whole phase space, including the remaining magnitudes (y_1 y_2, …, y_N), in the discrete form of the corresponding time series $(Y_1^{(k)}, Y_2^{(k)}, \ldots, Y_N^{(k)})$ by making $Y_i^{(k)} = Y_1^{(k+\Delta_i)}$ with i = 1,2,N and $\Delta_1 = 0$, where each non-negative integer Δ_i defines a time delay $t_{d_i} = t_{k+\Delta_i} - t_k = \Delta_i \cdot \tau$. Observe that the time delay does not depend on the measure number k because the time step τ is fixed. Namely, in terms of graphical representations, the phase space is reconstructed in a phase graph from a time series by means of the representation of such time series versus itself delayed in time, the appropriate value for the time delays t_{d_i} and system dimension N being obtained by heuristics. In this work, two-dimensional (N = 2) phase space representations have been obtained by plotting the measured temperature $T(k)$ at each time $t(k)$ versus the temperature $T(k + \Delta)$ at time $t(k + \Delta)$, with optimum Δ = 1 set up by heuristics. In this case, the data acquisition interval (i.e., the fixed time step of the time series) is τ = 71 min so that the corresponding time delay is td $t_d = \Delta \cdot \tau$ = 71 min. For obtaining the optimum time delay, different values of Δ have been systematically tested, looking for the maximum area of the trajectory loops in the phase space. The area of the trajectory loops corresponding to one sensor or group of sensors has been computed by using the Matlab® function *convhulln*. This function allows for selecting a set of points from the trajectory loop in the phase space plot and returns the smallest convex envelope containing the set of points and the corresponding area. Function *convhulln* is based on the Quickhull (Qhull) algorithm for convex hulls (Barber et al., 1996).

The software STATISTICA 6.1 (StatSoft, Inc.) and the statistical toolbox of Matlab® version 7.0 (R14) were used to compute basic statistics, such as the mean and standard deviation (SD), and to carry out the analysis of variance (ANOVA).

3 Results and discussion

3.1 Effect of spatial distribution

Figure 2 presents the dynamic of temperatures in the pallets, registered by RFID tags along the complete trip (i.e., LSS and SS). Taking into account all data of the 18 RFID tags, the average temperature of the batch of pallets of blueberries was 0.54ºC above the set point (–1ºC). The average of absolute minimum temperatures (n = 18 sensors) was

–1.5ºC, with –2ºC being the lowest registered temperature corresponding to one sensor located in the bottom of a pallet (layer 4), while the maximum absolute temperature (9.3ºC) was registered at the upper part of the pallet (layer 24), which is in accordance with the air flow in a bottom-air delivery reefer. Defrosting and door opening processes are also identified in the graph.

A one-way ANOVA was carried out to analyse the vertical temperature distribution in the pallet during the complete journey. This analysis showed that the distribution of load at different heights on the pallet had a significant effect ($F = 40.9$, $p < 0.05$), having a decreasing vertical temperature from the top of the pallet to the bottom (average temperature of 0.2ºC at 160 cm, –0.5 at 133 cm, –0.7 at 80 cm, –0.8 at 27 cm).

Figure 2 Dynamics of temperature in the pallets registered by the five groups of RFID tags (see online version for colours)

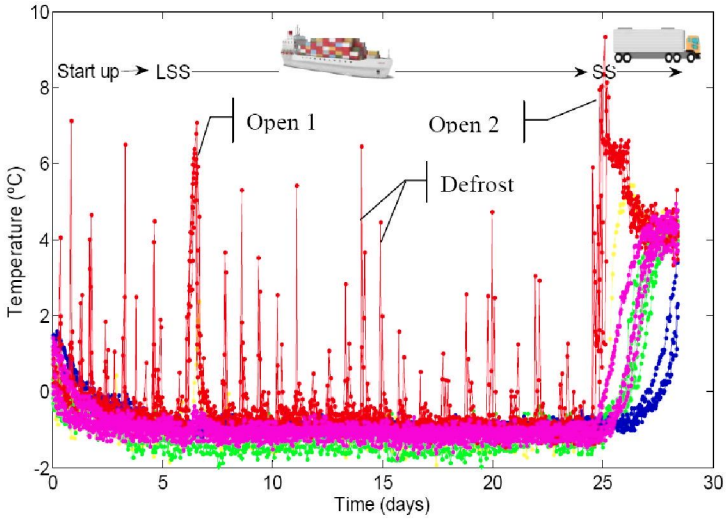

Notes: (18 sensors) resulting from cluster analysis. Group A: in red; group B: in yellow; group C: in magenta; group D: in dark blue; group E: in green. LSS: long sea shipping. SS: short shipping.

Table 3 Mean (M) and SD average of the temperature for the five sensor clusters for the entire journey

Sensor group	*Sensor id.*	*Layer*	*Temperature (ºC)*				*Area (ºC²)*		
			M	*±SD*	*Min*	*Max*	*Area*	*M*	*±SD*
A	4	24	0.19	2.1	–1.46	9.35	75.71	68.26	12.16
	7	24					56.24		
	9	24					81.34		
	12	24					59.76		
B	2	20	–21	_	–1.91	4.95	14.51	14.51	_

Notes: Area calculated on phase space representations of temperature is also shown. Min: group absolute minimum temperature, Max: group absolute maximum temperature.

Table 3 Mean (M) and SD average of the temperature for the five sensor clusters for the entire journey (continued)

Sensor group	*Sensor id.*	*Layer*	*Temperature (°C)*				*Area (°C²)*		
			M	*±SD*	*Min*	*Max*	*Area*	*M*	*±SD*
C	1	20	–0.57	1.32	–1.75	4.95	5.21	4.78	0.50
	6	20					4.63		
	13	20					5.35		
	10	12					4.11		
	14	8					4.59		
D	8	12	–0.7	0.56	–1.32	3.4	2.48	2.39	0.94
	16	12					2.39		
	15	8					2.30		
E	18	12	–0.73	1.18	–1.97	4.5	6.01	4.50	3.53
	3	4					4.04		
	5	4					4.28		
	11	4					4.63		
	17	4					3.53		

Notes: Area calculated on phase space representations of temperature is also shown.
Min: group absolute minimum temperature, Max: group absolute maximum temperature.

Figure 3 The temperature histograms for clusters A to E (see online version for colours)

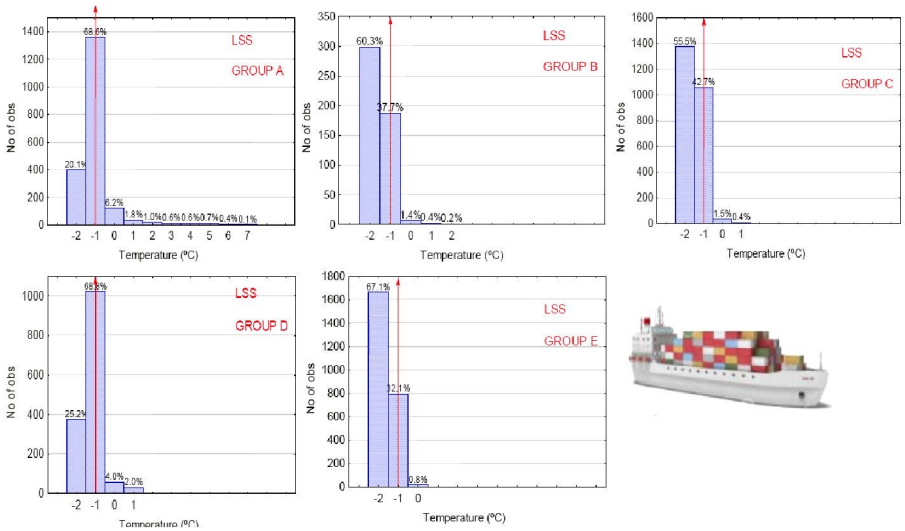

Notes: Corresponding to LSS (up) and SS (down). A much higher thermal variability of SS is found compared with LSS. Set-point (–1°C) is indicated by the red line.

Figure 3 The temperature histograms for clusters A to E (continued) (see online version for colours)

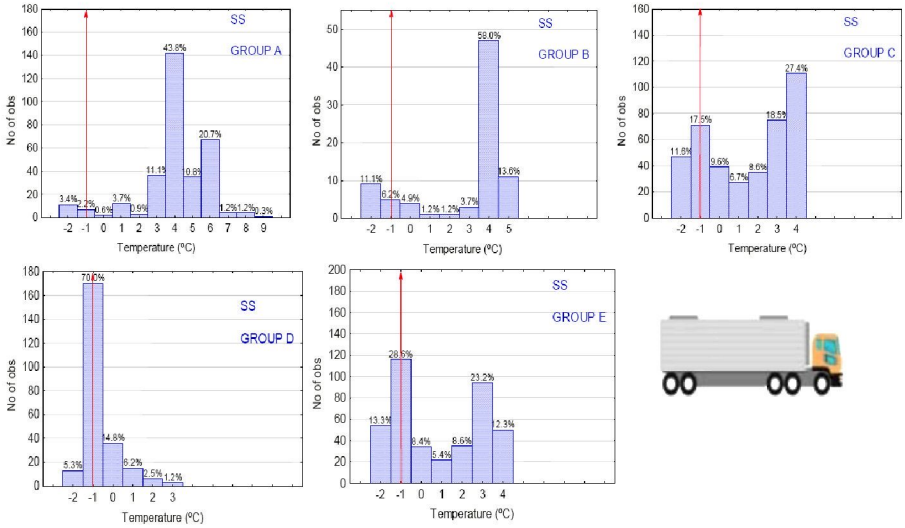

Notes: Corresponding to LSS (up) and SS (down). A much higher thermal variability of SS is found compared with LSS. Set-point (–1ºC) is indicated by the red line.

Figure 4 Phase diagram for temperature (see online version for colours)

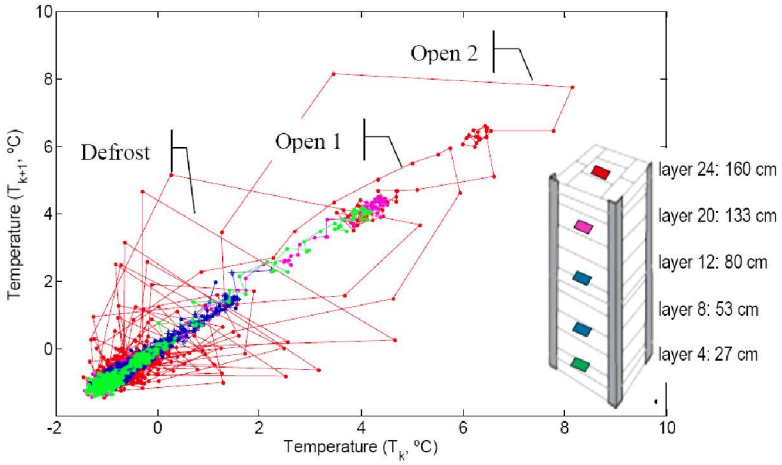

Notes: With $\Delta = 1$ ($t_d = 1$(step)·71(min/step) = 71min) for RFID tag sensors placed in the pallet no. 2 at different heights; sensor located at layer 24 belongs to group A, in red; sensor located at layer 20 belongs to group C, in magenta; sensors located at layers 12 and 8 belong to group D, in dark blue; sensor located at layer 4 belongs to group E, in green.

A clustering procedure was applied to the temperature profiles as referred to in materials and methods (Figure 2). The 18 RFID tags were clustered into five groups labelled from A to E. Table 3 characterises each group: group A, consisting of four RFID tags, corresponds to the hottest locations, i.e., in the upper part of the pallet (layer 24, 160-cm height); group B only includes one sensor at layer 20 (133 cm); group C includes five RFID tags located in the top half of the pallet (from 133 to 53 cm); group D includes three RFID tags located at the core of the pallet (from 80 to 53 cm); group E contains five sensors at the coldest locations, with the average temperature nearest to the set point, located at the bottom of the pallet (mainly placed at layer 4 at 24 cm above the floor). The one-way ANOVA carried out for these temperature groups showed significant differences ($F = 26.9$, $p < 0.05$).

By way of example, Figure 4 shows the phase space representation of the thermal series in pallet 2 for the entire journey ($\Delta = 1$, $= t_d$ 1(step)·71(min/step) = 71min). The areas (see Table 3) of the polygons that include all of the data points of each sensor on their phase spaces quantify the variability of the temperature at each location. The one-way ANOVA carried out showed that the difference in the average areas computed for each group (A to E) were significant ($F = 91.6$, $p < 0.05$).

Consequently, group A (red sensors in Figure 2 and Figure 4) corresponds to the hottest zone of the pallets and also to the most variable zone (68.3°C^2, $\Delta = 1$). Group E (green sensors) is near the set point (Figure 4) and provides the coldest points inside the pallets. This location, at the bottom of the pallets, showed minor temperature variations (average area of 4.5°C^2, $\Delta = 1$). Group D (blue sensors) identifies points at medium height of the pallet near the set point (average temperature –0.7°C), where the temperature is most stable (average area 2.4°C^2, $\Delta = 1$).

During LSS, sensors belonging to group A exhibited large cyclic thermal behaviour (Figure 2), corresponding to defrosting periods. Temperature oscillations caused by the defrosting cycles of the reefer unit are clearly remarked in the large loops that appear in the thermal phase graphs for the sensors that belong to group A (Figure 4, red sensor). The oscillations measured for sensor group A had a temperature increase of up to 5°C. groups B to E, located in the inner part of the pallets, were more or less out of the main airflow stream with further stable behaviour (more relevant to group D).

3.2 Effect of intermodal transport

Along LSS, the average SD (n = 18 sensors) was ±0.35°C, a value that was nearly double the accuracy of the sensors (±0.19°C) (Jedermann et al., 2009); in the same period, the average spatial SD computed for sensors at different locations for the same instant (n = 431 time data) reached a similar value (±0.37°C). Both values of SD increased by factors of 5.9 and 4.6 respectively during the SS in Europe (from Rotterdam to Verona, four days).

Figure 5 LS means graphs of temperature for the five groups of RFID tags during the LSS and SS stage (see online version for colours)

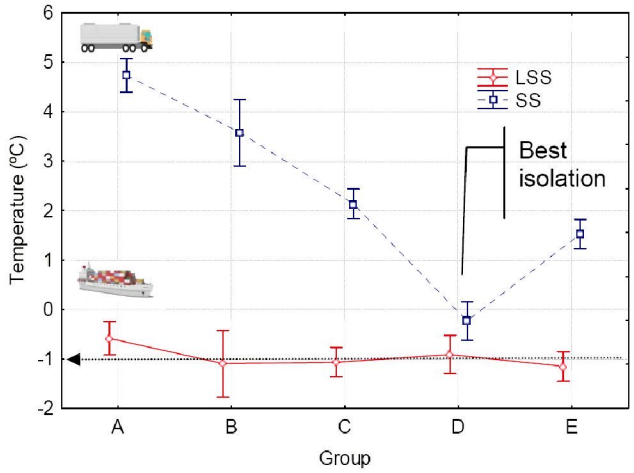

Notes: Vertical bars denote 0.95 confidence intervals. Set-point (–1ºC) is indicated by the black arrow.

A two-way ANOVA (Figure 5) was carried out to analyse the effect of: the spatial distribution of tags in the pallet (factor a) and the transport stage (factor b). Both factors were significant ($F_{a*b} = 47.4$, $p < 0.05$). The analysis showed that the transhipment of the container from the vessel to the truck had the highest effect ($F_b = 644.7$, $p < 0.05$), increasing significantly the temperature at all locations in the pallets, from an average temperature (n = 18 sensors) of –0.99 ± 0.35ºC for LSS to 2.23 ± 2.08ºC for SS. On the other hand, the height of the pallet also had significant impact ($F_a = 65.7$, $p < 0.05$). The main vertical gradient of temperature occurred during SS, with a higher temperature for the upper part (160 cm, group A) compared with the centre of the pallet (80 to 53 cm, group D). Between these two locations, the average temperature difference was 4.97ºC (from 4.74ºC group A to –0.23ºC group D), with a maximum instant variation of 9.1ºC between 160 cm and 80 cm for sensors located in the same pallet (maximum temperature gradient of 0.11ºC/cm of 0.8ºC/box layer).

Figure 6 shows the phase space representation of temperature series along the LSS and SS ($\Delta = 1$, $t_d = 1(\text{step}) \cdot 71(\text{min/step}) = 71$ min) for the five clusters (A to E). For each group, different patterns of the time series corresponding to LSS and SS were found. Thermal values registered during LSS (red lines in phase graphs of Figure 6) allow for the reconstruction of an attractor: the structure toward which a dynamic system tends, even when it is slightly disturbed, as occurred in group A during defrosting and group B during door opening. The change of transport modality makes that temperature undergo an abrupt and sustained change over time, modifying the trajectory of the dynamic system and its attractor (blue lines in phase graphs of Figure 6).

Figure 6 Phase diagrams for temperature (see online version for colours)

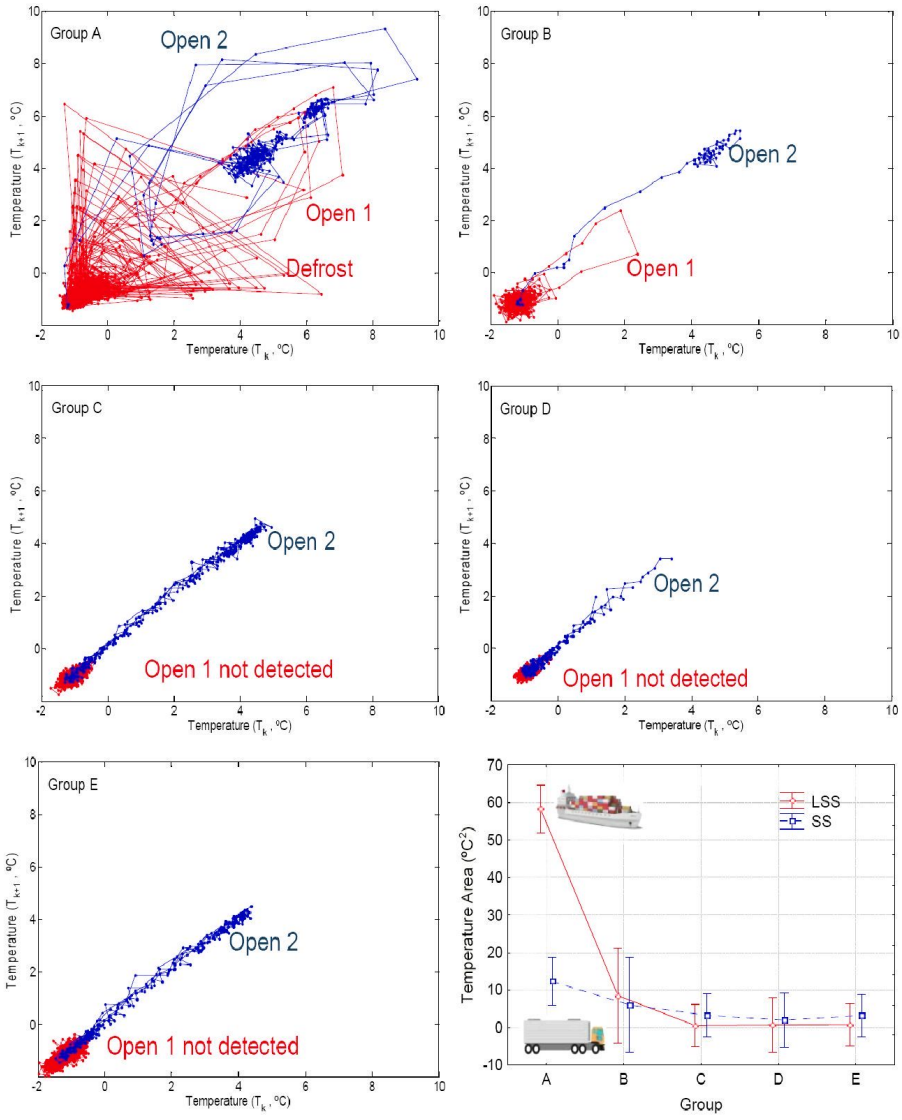

Notes: With $\Delta = 1$ ($t_d = 1$(step)·71(min/step) = 71min) for groups of RFID tag sensors from A to E, as well as for LSS (red line) and SS (blue line). Bottom right LS means graph of temperature area computed on phase diagrams for the five groups of RFID tags during the LSS and SS stage. Vertical bars denote 0.95 confidence intervals.

3.3 *Discussion*

The quality of the fresh blueberries is related not only to the storage temperature but also to the corresponding temporal variations. In this work, the maximum range of variation registered by the 18 RFID tags was 11.3ºC, with the maximum spatial range (same time instant, different location) being 9.1ºC, which occurred during SS. These ranges are in accordance with previous published data that reported deviations above 5ºC or more during long transports (Jedermann et al., 2009; Lang et al., 2011). According to Paniagua et al. (2014), it is unknown whether this type of temperature heterogeneity during shipping could constitute an important factor affecting final blueberry quality in the marketplace. These authors found that increases of 4ºC in storage temperature (with respect to a set point of 0ºC) resulted in more rot incidences, even when using controlled atmospheres as for the case of this study. In our work, SS was characterised by the highest average temperature (2.23ºC), the highest temporal variation (2.08ºC of average SD) and the highest spatial variation, showing a vertical gradient of 5ºC. During SS, blueberries located at the highest location in pallets would be the most stressed (highest values of area in the phase graphs) and thus these fruits would be most susceptible to rotting.

On the other hand, it is interesting to remark that the set point of –1ºC selected for this transport is below the recommended temperature of 0ºC to store fresh blueberries (Paniagua et al., 2014; Zhou et al., 2014). According to Paniagua et al. (2014), blueberries stored for 30 days at 0ºC pitted after two days at room temperature. External pitting is a symptom of chilling injury on fruits that could affect the blueberries transported under a LSS stage of 22 days under an average temperature of –0.99ºC. The sensors of Group E (coldest locations, average temperature –1.2ºC during LSS) would be characterising the location at highest risk of fruit chilling injury.

The built-in sensors of a standard refrigeration unit measure only the inlet and outlet air temperature and not the freight temperature (Lang et al., 2011); indeed, as stated by Jedermann and Lang (2014), in most cases, the provided temperature data are only checked for maximum or average temperature. In this transport, the average temperature (n = 18 sensors) of the batch of pallets of blueberries for the complete journey was –0.46ºC, which is within the recommended values of the set point ±0.5ºC (Jedermann et al., 2009; James et al., 2006). Taking into account only the average temperature, this shipping could be qualified as fit.

During SS, the average temperature (n = 18 sensors) rose to 3.22ºC with respect to the average registered during LSS (–0.99ºC), while the average SD was six times higher. As the authors found in previous works (Jiménez-Ariza et al., 2014), the change in transport modality either from ship to ship or ship to truck, as in this case, increases temperature heterogeneity, becoming a critical point in the logistics process. While the loading transfer from ship to ship doubled the SD, in the case of ship to truck the average sensor variability increased six-fold. The temperature faulty management could be due to the truck driver turning off the cooling unit during rest time to save fuel and/or to different personnel having different instructions about the consigned set points at different points in the cold chain (such as ship crew versus harbour crew versus truck driver) (Jedermann and Lang, 2014).

From the phase space representation, it is possible to extract information from the time series by pattern recognition of the attractors, as was applied before (Jimenez-Ariza, 2014). In such study, several behaviours were found for the long ship transport stage of a

lemons reefer compared with short ship after container transhipment. As was stated by Jiménez-Ariza et al. (2014) and as shown here in Figure 6, the trajectories of the dynamic system present identifiable shapes, also referred to as attractors, for the different periods during transport. On the other hand, the areas computed on phase graphs provide an idea of the thermal stress (Villarroel et al., 2011) (temporal gradients of temperature), to which the fruits were subjected during the journey. The transfer of the container from the ship to the truck increases the area on the phase graph by 1.2 in sensors located at the upper part of the pallets, which were most exposed to the main return of the air flow. A similar result was found by Jiménez-Ariza et al. (2014), where the area on the phase graph computed for one sensor located at the return of the cold unit increased by 6.5 when the container was transferred from vessel to vessel after several days of waiting in the harbour.

In this work, the spatial distribution of the cargo regarding the pallet height had a significant effect on temperature variability. The phase graph areas computed for sensors located in the upper part of the pallet were, on average, ten times higher than those computed for sensors located in the core (53–80 cm above the floor); this was mainly due to the large thermal inertia (Jedermann et al., 2009) and because the pallets were out of the main delivery and return airflow.

The supervised shipment was a commercial transport carried out under real conditions. In this case and as stated by Jedermann et al. (2014), the freight consolidation process could have a negative effect on the shelf life because it is not possible to adjust the set point to the optimal temperature for all of the products in a mixed container, as was used in this transport of blueberries. On the other hand, when the pallets of blueberries arrived to Verona (Italy), the cargo owner did not declare any damage or decay in the fruits. However, it is known that accumulated exposure to higher than planned temperatures resulted in 'physically invisible' advanced shelf life loss. Common hands-on visual inspection does not show the accumulated shelf life loss (Jedermann et al., 2014), but the quality can rapidly deteriorate when fruit is moved to shelf conditions at ambient temperature (Zhou et al., 2014).

4 Conclusions

Temperature gradients inside refrigeration rooms, containers and trucks are a primary concern of the fresh food industry. The phase space diagram of temperatures emphasises the differences between the temperatures recorded by the sensors at different times and locations. Basic statistics such as the mean and SD are not able to compute the occurrence of cycles or temperature variations that are highlighted in the phase space. The area calculated on phase diagrams of temperature is a new parameter that allows for avoiding such limitation.

Five groups of sensors have been identified as characterising temperature behaviour in the pallets at different heights along the transportation process (expressed as Temperature and Area in the phase space). The thermal variability (area in the phase space) of a sensors cluster has higher impact ($F = 91.6$, $p < 0.05$) than the temperature itself ($F = 26.9$, $p < 0.05$), indicating the relevance of the dynamic analysis. A main conclusion of this work is the importance of combining data visualisation techniques with new statistical features to allow for faulty diagnosis with a hacked eye: useful for either trained or untrained operators.

Acknowledgements

We thank the enterprise FIELD SA (Uruguay) and its staff for technical help in loading and unloading operations and in the placement of sensors. This study was funded by the Spanish Government through the SMART-QC project (GL2008-05267-C03-03), Comunidad de Madrid-Structural Funds of the European Union S2013/ABI-2747 (TAVS-CM) and FRUTURA (109RT0383) International Net of CYTED. We also thank them for their support to the Technical University of Madrid and the International Campus of Excellence CEI Moncloa/UPM-UCM.

References

Barber, C.B., Dobkin, D.P. and Huhdanpaa, H. (1996) 'The quickhull algorithm for convex hulls', *ACM Trans. Math. Softw.*, Vol. 22, No. 4, pp.469–483.

Correa, E.C., Jiménez-Ariza, T., Diaz-Barcos, V., Barreiro, P., Diezma, B., Oteros, R., Echeverri, C., Arranz, F.J. and Ruizaltisent, M. (2014) 'Advanced characterisation of a coffee fermenting tank by multi-distributed wireless sensors: spatial interpolation and phase space graphs', *Food and Bioprocess Technology*, Vol. 7, No. 11, pp.3166–3174.

Costa, C., Antonucci, F., Pallottino, F., Aguzzi, J., Sarria, D. and Menesatti, P. (2013) 'A review on agri-food supply chain traceability by means of RFID technology', *Food and Bioprocess Technology*, Vol. 6, No. 2, pp.353–366.

Dabbene, F., Gay, P. and Tortia, C. (2014) 'Traceability issues in food supply chain management: a review', *Biosystems Engineering*, No. 120, pp.65–80.

Eckmann, J.P. and Ruelle, D. (1985) 'Ergodic-theory of chaos and strange attractors', *Reviews of Modern Physics*, Vol. 57, No. 3, pp.617–656.

FAO (2014) *Pérdidas y Desperdicios de Alimentos en América Latina y el Caribe*, Chile.

Garcia, M.R., Vilas, C., Banga, J.R. and Alonso, A.A. (2007) 'Optimal field reconstruction of distributed process systems from partial measurements', *Industrial & Engineering Chemistry Research*, Vol. 46, No. 2, pp.530–539.

Gustavsson, J., Cederberg, C., Sonesson, U., van Otterdijk, R. and Meybeck, A. (2011) 'Global food losses and food waste', *SAVE FOOD!*, FAO, Düsseldorf, Germany.

James, S.J., James, C. and Evans, J.A. (2006) 'Modelling of food transportation systems – a review', *International Journal of Refrigeration*, Vol. 29, No. 6, pp.947–957.

Jedermann, R. and Lang, W. (2014) 'Model based estimation of biological heat generation during coldchain transport and processing', *3rd IIR International Conference on Sustainability and the Cold Chain*, pp.86–93.

Jedermann, R., Geyer, M., Praeger, U. and Lang, W. (2013) Sea transport of bananas in containers – parameter identification for a temperature model', *Journal of Food Engineering*, Vol. 115, No. 3, pp.330–338.

Jedermann, R., Nicometo, M., Uysal, I. and Lang, W. (2014) 'Reducing food losses by intelligent food logistics', *Philosophical Transactions of the Royal Society a-Mathematical Physical and Engineering Sciences*, Vol. 372, No. 2017, p.20130302.

Jedermann, R., Ruiz-Garcia, L. and Lang, W. (2009) 'Spatial temperature profiling by semi-passive RFID loggers for perishable food transportation', *Computers and Electronics in Agriculture*, Vol. 65, No. 2, pp.145–154.

Jiménez-Ariza, T., Correa, E.C., Diezma, B., Silveira, A.C., Zocalo, P., Arranz, F.J., Moya-Gonzalez, A., Garrido-Izard, M., Barreiro, P. and Ruiz-Altisent, M. (2014) 'The phase space as a new representation of the dynamical behaviour of temperature and enthalpy in a reefer monitored with a multidistributed sensors network', *Food and Bioprocess Technology*, Vol. 7, No. 6, pp.1793–1806.

Lang, W., Jedermann, R., Mrugala, D., Jabbari, A., Kriegbrueckner, B. and Schill, K. (2011) 'The 'intelligent container' – a cognitive sensor network for transport management', *IEEE Sensors Journal*, Vol. 11, No. 3, pp.688–698.

Packard, N.H., Crutchfield, J.P., Farmer, J.D. and Shaw, R.S. (1980) 'Geometry from a time-series', *Physical Review Letters*, Vol. 45, No. 9, pp.712–716.

Paniagua, A.C., East, A.R. and Heyes, J.A. (2014) 'Interaction of temperature control deficiencies and atmosphere conditions during blueberry storage on quality outcomes', *Postharvest Biology and Technology*, No. 95, pp.50–59.

Rodriguez-Bermejo, J., Barreiro, P., Robla, J.I. and Ruiz-Garcia, L. (2007) 'Thermal study of a transport container', *Journal of Food Engineering*, Vol. 80, No. 2, pp.517–527.

Villarroel, M., Barreiro, P., Kettlewell, P., Farish, M. and Mitchell, M. (2011) 'Time derivatives in air temperature and enthalpy as non-invasive welfare indicators during long distance animal transport', *Biosystems Engineering*, Vol. 110, No. 3, pp.253–260.

Zhou, Q., Zhang, C., Cheng, S., Wei, B., Liu, X. and Ji, S. (2014) 'Changes in energy metabolism accompanying pitting in blueberries stored at low temperature', *Food chemistry*, No. 164, pp.493–501.